Wide spectral range confocal microscope based on endlessly single-mode fiber

R. Hubbard[1,2], Yu. B. Ovchinnikov[1], J. Hayes[3], D. J. Richardson[3], Y. J. Fu[4], S.D. Lin[4], P. See[1], and A.G. Sinclair[1*]

[1]*National Physical Laboratory, Hampton Road, Teddington, Middlesex, TW11 0LW, UK*
[2]Blackett Laboratory, Imperial College London, Prince Consort Road, London SW7 2BW, UK
[3]*Optoelectronics Research Centre, University of Southampton, Southampton S017 1BJ, UK*
[4]*Department of Electronic Engineering, National Chiao Tung University, Hsinchu 300, Taiwan*
**alastair.sinclair@npl.co.uk*

Abstract: We report an endlessly single mode, fiber-optic confocal microscope, based on a large mode area photonic crystal fiber. The microscope confines a very broad spectral range of excitation and emission wavelengths to a single spatial mode in the fiber. Single-mode operation over an optical octave is feasible. At a magnification of 10 and λ = 900 nm, its resolution was measured to be 1.0 μm (lateral) and 2.5 μm (axial). The microscope's use is demonstrated by imaging single photons emitted by individual InAs quantum dots in a pillar microcavity.

OCIS codes: (180.1790) Confocal microscopy; (110.2350) Fiber optics imaging; (060.4005) Microstructured fibers; (300.6470) Spectrsocopy, semiconductors; (270.5290) Photon statistics.

References and links

1. J. B. Pawley, *Handbook of Biological Confocal Microscopy, Third Edition*, (Springer, New York 2005).
2. C. W. Hoheisel, W. Jacobsen, B. Lüttge, and W. Weiner, "Confocal microscopy: applications in materials science," Macromol. Mater. Eng. **286**(11), 663–668 (2001).
3. A. J. Shields, "Semiconductor quantum light sources," Nat. Photonics **1**(4), 215–223 (2007).
4. M. Oxborrow, and A. G. Sinclair, "Single-photon sources," Contemp. Phys. **46**(3), 173–206 (2005).
5. C. Santori, M. Pelton, G. Solomon, Y. Dale, and Y. Yamamoto, "Triggered single photons from a quantum dot," Phys. Rev. Lett. **86**(8), 1502–1505 (2001).
6. C. Kurtsiefer, S. Mayer, P. Zarda, and H. Weinfurter, "Stable solid-state source of single photons," Phys. Rev. Lett. **85**(2), 290–293 (2000).
7. M. Minsky, "*Microscopy Apparatus*", U.S. patent 3,013,467 (1961).
8. M. R. Harris, "*Scanning confocal microscope including a single fiber for transmitting light to and receiving light from an object*", U.S. patent 5,120,953 (1992).
9. W. Denk, J. H. Strickler, and W. W. Webb, "Two-photon laser scanning fluorescence microscopy," Science **248**(4951), 73–76 (1990).
10. K. Shi, P. Li, S. Yin, and Z. Liu, "Chromatic confocal microscopy using supercontinuum light," Opt. Express **12**(10), 2096–2101 (2004).
11. A. R. Rouse, and A. F. Gmitro, "Multispectral imaging with a confocal microendoscope," Opt. Lett. **25**(23), 1708–1710 (2000).
12. N. Uzunbajakava, and C. Otto, "Combined Raman and continuous-wave-excited two-photon fluorescence cell imaging," Opt. Lett. **28**(21), 2073–2075 (2003).
13. A. M. Gigler, A. J. Huber, M. Bauer, A. Ziegler, R. Hillenbrand, and R. W. Stark, "Nanoscale residual stress-field mapping around nanoindents in SiC by IR s-SNOM and confocal Raman microscopy," Opt Express **17**(25), 22351–22357 (2009).
14. T. Gaebel, I. Popa, A. Gruber, M. Domhan, F. Jelezko, and J. Wrachtrup, "Stable single-photon source in the near infrared," N. J. Phys. **6**, 98 (2004).
15. C. Santori, D. Fattal, J. Vuckovic, G. S. Solomon, and Y. Yamamoto, "Single-photon generation with InAs quantum dots," N. J. Phys. **6**, 89 (2004).
16. A. J. Bennett, D. C. Unitt, P. Atkinson, D. A. Ritchie, and A. J. Shields, "High performance single photon sources from photolithographically defined pillar microcavities," Opt. Express **13**(1), 50–55 (2005).
17. T. Aichele, V. Zwiller, and O. Benson, "Visible single-photon generation from semiconductor quantum dots," N. J. Phys. **6**, 90 (2004).
18. T. A. Birks, J. C. Knight, and P. St. J. Russell, "Endlessly single-mode photonic crystal fiber," Opt. Lett. **22**(13), 961–963 (1997).
19. N. A. Mortensen, M. D. Nielsen, J. R. Folkenberg, A. Petersson, and H. R. Simonsen, "Improved large-mode-area endlessly single-mode photonic crystal fibers," Opt. Lett. **28**(6), 393–395 (2003).

#131463 - $15.00 USD Received 13 Jul 2010; revised 6 Aug 2010; accepted 11 Aug 2010; published 18 Aug 2010

20. W. Denk, D. W. Piston, and W. W. Webb, "Multi-photon molecular excitation in laser-scanning microscopy," in *Handbook of Biological Confocal Microscopy, Third Edition*, J.B. Pawley, ed. (Springer, New York 2005).
21. F. Helmchen, D. W. Tank, and W. Denk, "Enhanced two-photon excitation through optical fiber by single-mode propagation in a large core," Appl. Opt. **41**(15), 2930–2934 (2002).
22. D. G. Ouzounov, K. D. Moll, M. A. Foster, W. R. Zipfel, W. W. Webb, and A. L. Gaeta, "Delivery of nanojoule femtosecond pulses through large-core microstructured fibers," Opt. Lett. **27**(17), 1513–1515 (2002).
23. K. Carlson Maitland, H.-J. Shin, H. Ra, D. Lee, O. Solgaard, and R. Richards-Kortum, "Single fiber confocal microscope with a two-axis gimbaled MEMS scanner for cellular imaging," Opt. Exp. **14**, 8604–8612 (2006).
24. J. C. Baggett, T. M. Monro, K. Furusawa, V. Finazzi, and D. J. Richardson, "Understanding bending losses in holey optical fibers," Opt. Commun. **227**, 317–335 (2003).
25. A. Högele, S. Seidl, M. Kroner, K. Karrai, C. Schulhauser, O. Sqalli, J. Scrimgeour, and R. J. Warburton, "Fiber-based confocal microscope for cryogenic spectroscopy," Rev. Sci. Instrum. **79**(2), 023709 (2008).
26. M. Pelton, C. Santori, J. Vucković, B. Zhang, G. S. Solomon, J. Plant, and Y. Yamamoto, "Efficient source of single photons: a single quantum dot in a micropost microcavity," Phys. Rev. Lett. **89**(23), 233602 (2002).
27. P. Stavrinou, Department of Physics, Imperial College London, London SW7 2AZ (personal communication, 2008).
28. R. P. Mirin, "Photon antibunching at high temperature from a single InGaAs/GaAs quantum dot," Appl. Phys. Lett. **84**(8), 1260–1262 (2004).
29. J. J. Finley, A. D. Ashmore, A. Lemaître, D. J. Mowbray, M. S. Skolnick, I. E. Itskevich, P. A. Maksym, M. Hopkinson, and T. F. Krauss, "Charged and neutral exciton complexes in individual self-assembled In(Ga)As quantum dots," Phys. Rev. B **63**(7), 073307 (2001).
30. C. Becher, A. Kiraz, P. Michler, A. Imamoglu, W. V. Schoenfeld, P. M. Petroff, L. D. Zhang, and E. Hu, "Nonclassical radiation from a single self-assembled InAs quantum dot," Phys. Rev. B **63**(12), 121312 (2001).

1. Introduction

Confocal microscopy is used in a variety of scientific disciplines, ranging from biology [1] to materials science [2]. In physics, optical detection of individual emitters is a widely used technique in various areas of quantum optics and quantum information science [3]. Single-photon sources [4] rely on the ability to maximally resolve a single emitter from any others nearby. In the case of solid-state systems such as quantum dots [5] or color centers [6], a confocal microscope is used to image an individual emitter. The original confocal microscope concept [7] uses a pinhole to define the small point in space to be imaged, enabling 2D and 3D images to be constructed via scanning. In a fiber-optic confocal microscope [8], the fiber core is analogous to the pinhole of a conventional system. By using a single-mode optical fiber, the excitation laser is delivered to the sample in a single spatial mode, and can be focused to a diffraction-limited spot, thus maximizing the instrument's resolution. The fluorescent photons are also guided in a single spatial mode by the fiber, making it straightforward to manipulate these photons efficiently in any subsequent optical system. For many quantum-optical applications, it is essential that these photons occupy a single spatial mode.

In the context of wider applications, it is desirable to be able to operate such an instrument over a range of wavelengths. For example, in two-photon microscopy [9], there is a significant difference between the wavelengths of the absorbed pump (λ_p) and emitted fluorescence (λ_{em}) photons. Chromatic confocal microscopy relies on broadband illumination (e.g. the visible part of a supercontinuum) and detection [10]. Multispectral confocal microscopy also detects across a range of wavelengths, frequently as wide as the visible spectrum [11]. Confocal Raman microscopy [12,13] constructs chemical images of samples, and benefits from operation at various different wavelengths. Where the Raman signal is compromised by fluorescence, it is practical to have access to several laser wavelengths (e.g. 532 nm, 633 nm, 785 nm) within the microscope to maximize the Raman signal detected with the microscope.

There are many systems of solid-state single emitters, and collectively their pump and fluorescence wavelengths are spread over a wide range. In addition, for any specific system, the difference between λ_p and λ_{em} can often be large. For a single NV color centre in diamond λ_p = 532 nm and λ_{em} = 637 nm (zero-phonon line); at room temperature λ_{em} peaks at ~680 nm and extends out to ~740 nm [6]. Also in diamond, the NE8 color centre operates with λ_p = 700 nm and λ_{em} = 802 nm [14]. In photoluminescence (PL) studies of InAs quantum dots emitting around 900 nm, near-resonant excitation uses $\left(\lambda_{em} - \lambda_p\right) \leq 30\,\text{nm}$, while above band

#131463 - $15.00 USD Received 13 Jul 2010; revised 6 Aug 2010; accepted 11 Aug 2010; published 18 Aug 2010

excitation can easily extend to $\left(\lambda_{em} - \lambda_p\right) \sim 200\,\text{nm}$ [5,15,16]. Quantum dots of CdSe and InP emit around λ_{em} = 510 nm and λ_{em} = 690 nm respectively [17], illustrating the spread of characteristic emission wavelengths across different systems that have been studied.

While optics such as mirrors and achromatic lenses are available for wide ranges of wavelengths, conventional single-mode fibers are not single mode over the full extent of these ranges. As an example, standard commercial components (e.g. mirrors, lenses) are typically available in the ranges of: $400\,\text{nm} \le \lambda_1 \le 700\,\text{nm}$, $650\,\text{nm} \le \lambda_2 \le 1050\,\text{nm}$, and $1050\,\text{nm} \le \lambda_3 \le 1620\,\text{nm}$. However, to operate a single mode fiber-optic confocal microscope, three fibers would be required to cover each range λ_1 and λ_2, necessitating fiber changes with wavelength. This is inconvenient during the study of a single sample, since it will most likely result in a change of the specific imaged volume, and could also require realignment of the instrument. A large mode area photonic crystal fiber, endlessly single-mode over a huge range of wavelengths [18,19], can be used to solve this problem. This paper presents the design, characterization and operation of a fiber-optic confocal microscope based on an endlessly single-mode photonic crystal fiber (PCF). Its use in PL spectroscopy of single semiconductor quantum dots is demonstrated.

The fiber microscope concept presented in this paper could be suitable for multi-photon confocal microscopy [20], a technique usually performed with high peak power sub-ps pulses. Normally this is performed with free-space optical paths; by using conventional single-mode fiber to deliver the excitation light, the pulses broaden unacceptably due to self-phase modulation. Attempts to reduce the effect to acceptable levels have used fibers of larger mode area (10 - 25 μm diameter) [21,22]. These investigations were successful in demonstrating a significant reduction in the temporal broadening of ultrashort pulses propagating in large mode area fibers, when compared with conventional single-mode fibers. Additionally [21], showed a corresponding improvement in two-photon excitation efficiency at the fiber output. However, the fibers used in these investigations were not single-mode, although they were operated at short lengths to minimize the coupling into higher order modes. In our approach, the mode area of the endlessly single-mode PCF can be sufficiently large to reduce the effects of self-phase modulation (as in [21,22]), whilst maintaining single-mode operation and tolerable bend loss over a wide range of wavelengths. The microscope presented here could allow fiber delivery of the excitation light in a true single mode, with reduced pulse broadening, for multiphoton microscopy. Chromatic confocal microscopy [10] is a technique that could also be fiber-enabled through the use of the endlessly single-mode PCF.

2. Microscope design

The confocal microscope, designed for imaging PL of semiconductor samples in a continuous-flow He cryostat, consists of several components (see Fig. 1a): 1) a scanning head contains the optics to focus the excitation laser onto the sample and image the PL onto the confocal aperture, 2) a large mode area PCF core is the confocal aperture, and guides the excitation laser to the sample and the PL to the detection apparatus, 3) a long-pass filter combines the beam paths of the excitation laser and the PL, 4) an imaging spectrometer detects and/or filters the emitted spectrum, 5) single-photon counting avalanche photodiodes (SPADs) analyze the quantum statistics of the emitted PL.

#131463 - $15.00 USD Received 13 Jul 2010; revised 6 Aug 2010; accepted 11 Aug 2010; published 18 Aug 2010

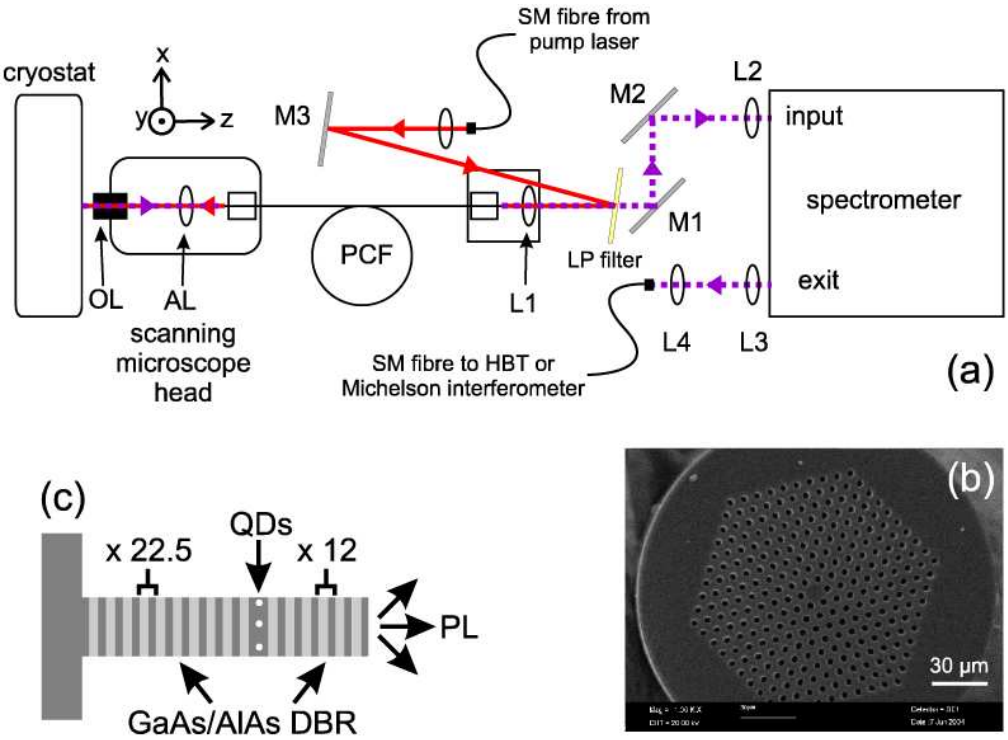

Fig. 1. a) Schematic setup of microscope apparatus. Pump laser light is delivered by a single-mode fiber. The microscope imaging head consists of an aspheric objective lens OL (f = 4.5 mm, NA = 0.55) and an achromatic coupling lens AL (f = 45 mm). PCF: photonic crystal fiber. LP: long pass filter. M1, M2, M3: high reflectors. L1, L2, L3, L4: achromatic lenses. An EMCCD (not shown) detects the imaged spectrum on the side exit of the spectrometer. Light filtered by the front exit slit is coupled to a single-mode fiber, and detected using either Hanbury Brown & Twiss or Michelson interferometers. b) Electron microscope image of large mode area PCF. (c) Schematic diagram of quantum dots (QDs) in a semiconductor DBR microcavity. The microscope objective focuses the excitation laser into the sample and the collects the photoluminescence (PL).

The cryostat is relatively bulky, and so remains in a fixed position, holding the sample (Fig. 1c) under study at a constant point in space. The imaging head of the microscope consists of the imaging optics and the PCF, which are all fixed with respect to each other. The microscope's imaging head was mounted on an x-y-z scanning stage, with piezo adjusters enabling a raster scan of up to 25 μm in each direction. While this is a simple construction, it is noted that miniaturized optical devices have been developed to scan the imaged volume in cellular imaging applications [23]. The optical fiber facilitates a flexible optical coupling between the scanning imaging head of the microscope and the fixed alignment of the detection apparatus. A primary requirement for the imaging optics was to maximize the collection efficiency of photons with $\lambda_{em} \sim 900\,\text{nm}$, yet maintain the working distance at a few mm as dictated by the flow cryostat. Long working distance microscope objective lenses with high NA are available for infrared wavelengths (and are expensive), however the many elements of the lens compromise their transmission. In this instance, an aspheric lens (Geltech 350230, with f = 4.5mm, NA = 0.55, working distance of 2.9 mm, and AR-coated for λ_2) is used, due to its transmission of >99% and relatively high NA. The second lens, termed the coupling lens (it couples light to and from the PCF), is an achromatic doublet (Thorlabs AC254-045-B, with f = 45 mm). The chromatic aberration introduced by the aspheric objective lens is not a limiting factor for our specific application. In principle this lens can be replaced by an infrared objective lens or an achromat; in the latter the NA will be smaller however this is only a significant compromise at very low fluxes of PL photons. For

#131463 - $15.00 USD Received 13 Jul 2010; revised 6 Aug 2010; accepted 11 Aug 2010; published 18 Aug 2010

applications at visible wavelengths, high quality microscope objectives are readily available, including those for long working distances. The lenses used here result in a magnification M = 10.

In cross-section, the large mode area PCF (see Fig. 1b) consists of a solid silica core surrounded by a lattice of many small holes running the length of the fiber. The fiber has a diameter of 193 μm, a hole spacing of 7.5 μm, with a hole diameter to pitch ratio of 0.46 which provides a mode field diameter of 9 μm and a critical bend radius of 2 cm at λ = 532 nm (where the critical bend radius is defined as the radius that produces 3 dB loss for one complete turn). The hole and pitch dimensions of the cladding determine its effective refractive index, which is strongly wavelength dependent. This enables single mode propagation across the full visible and NIR spectrum. Note that maintaining the short wavelength bend-losses associated with large-mode area PCF to a practical level is challenging and requires a careful choice of hole and pitch parameters [24]. A fiber length of ~2.0 m was used, to enable flexible movement of the scanning head on the table. An achromatic lens (Thorlabs AC127-030-B, f = 30 mm) collimates the PL as it emerges from the fiber towards the detection apparatus. A long-pass filter, transmitting λ_{em}, and reflecting λ_p, is used to combine the beam paths of the two counter-propagating radiations at λ_{em} and λ_p. For the application reported in this work, long pass filters at 850 nm and 900 nm (Omega Optical 3RD850LP & 3RD900LP) were used at a small incidence angle. Filters are readily available at a great variety of cut-on wavelengths. Unlike the PCF, they are straightforward to exchange in the apparatus, without significant effect on the alignment of the PL beam path. In our instance, the pump laser is delivered to the microscope by a single-mode fiber; where the application requires a pulsed source with high peak powers, a large mode area PCF can be used instead. To align the imaging optics, a pinhole of 2 μm diameter is illuminated with a laser (λ ~900 nm) and imaged onto the fiber core. Maximizing the light coupled into the fiber optimizes the alignment. With the imaging lens system (M = 10) described above, and the PCF with mode field diameter of 9 μm, the imaged spot diameter is 0.9 μm.

After transmission through the long-pass filter, the beam of PL photons is focused onto the entrance slit of the imaging spectrometer using an achromatic lens (f = 100 mm). This maximized transmission through the 40 μm entrance slit without exceeding the NA of the instrument. The spectrometer (Horiba Jobin Yvon iHR 550) has a 550 mm focal length and contains three gratings; a 1200 lines/mm grating blazed at 900 nm was used in the investigations reported here. An electron-multiplying CCD camera (Andor Newton DU971N-FI) recorded PL spectra on the side exit port. The camera is sensitive enough to record the spectrum from a single quantum dot with integration times of less than a second. The spectrometer's front exit slit is used to filter the PL photons in a narrow band (typically 0.11 nm) and transmits the desired spectral feature. These transmitted PL photons are coupled into a single-mode fiber, which is then directed towards the apparatus used to determine their coherence properties. Quantum statistics of the PL photons are analyzed by measuring the degree of second order coherence, $g^{(2)}(\tau)$, using a Hanbury Brown & Twiss correlator. Coherence time τ_c is measured using a Michelson interferometer. In both cases, fiber-coupled SPADs (Perkin Elmer SPCM-AQR-14-FC) are used to detect the photons.

3. Microscope characterization

The microscope's lateral resolution was investigated by acquiring a raster scan image of a razor blade edge and a pinhole aperture, each illuminated uniformly from behind with laser light at 935 nm. The laser light was highly attenuated, since a single APD was used to detect light transmitted through the microscope. Figure 2a shows a cross section of the measured intensity in a raster scan image of an illuminated razor blade edge. The spatial extent over which intensity rises from 10% to 90% is one means of quantifying resolution [23]. Applying this criterion to Fig. 2a yields a resolution of 1.1 μm. Alternatively, following the approach of [25], the gradient of this intensity profile is shown in Fig. 2b. Fitting a Gaussian profile to this yields a $1/e^2$ full width of 0.95 μm. Diffraction effects and experimental noise cause the non-uniform detected intensity in the range 4.5-7 μm (Fig. 2a), which in turn is responsible for the

#131463 - $15.00 USD Received 13 Jul 2010; revised 6 Aug 2010; accepted 11 Aug 2010; published 18 Aug 2010

noise in the measured intensity gradient, evident in the same range of Fig. 2b. These resolution values are close to the 0.9 μm expected from the PCF mode field diameter and the lens system magnification. The image of a circular pinhole, with diameter specified to be (10 ± 1) μm, was constructed by raster-scanning the microscope imaging head. The cross-section intensity profile had a diameter of 8.3 μm at FWHM, and 9.5 μm at 10% of the maximum. This is broadly in line with the lower limit of the pinhole's specified diameter. To measure the microscope's axial resolution [23], 900 nm laser light propagating in the fiber was focused by the objective lens onto a mirror in the focal plane, reflected back into the fiber, and detected by the SPADs. The microscope imaging head was scanned in the axial direction and the detected count rate recorded (Fig. 2c), yielding a FWHM axial resolution of 2.5 μm.

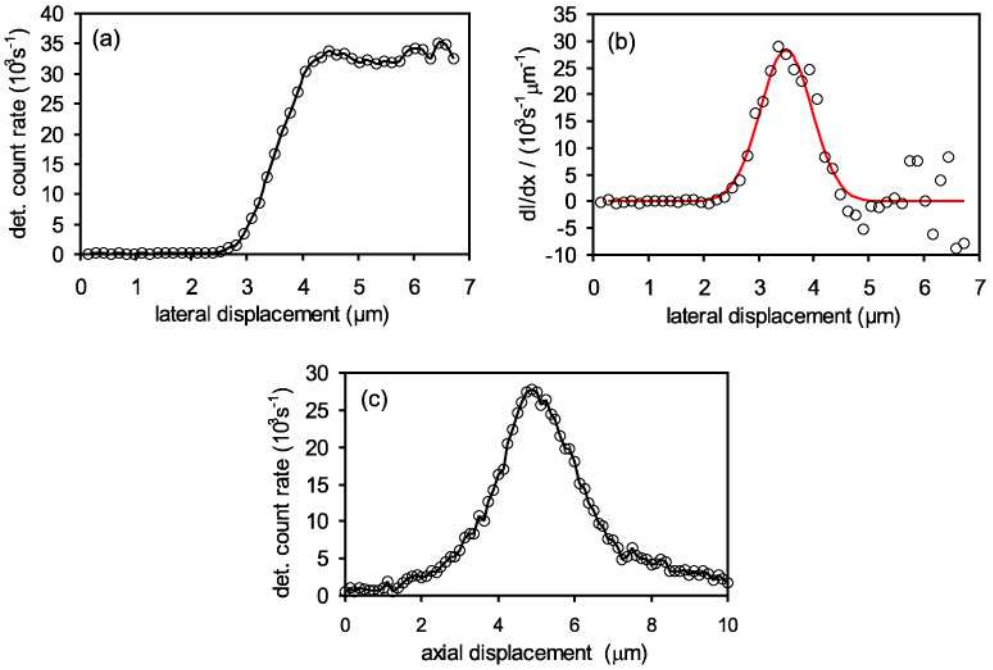

Fig. 2. Measurements of lateral and axial resolution. a) Cross-sectional intensity profile of raster scan image of an illuminated sharp edge. b) Derivative of intensity profile, *dI/dx*. The fitted Gaussian has a full width (at $1/e^2$) of 0.95 μm, which quantifies the microscope's lateral resolution. c) Signal detected when laser light is focused onto a mirror and its axial position is scanned through the focal plane. The signal's FWHM is 2.5 μm, and is a measure of the axial resolution.

The microscope's transmission was evaluated by imaging a pinhole (diameter of 2 ± 0.5 μm) illuminated by tightly focused laser light at either 900 nm or 935 nm. When optimally aligned, 54% of the light emerging from the pinhole was coupled into the PCF. The pinhole's non-uniform illumination is thought to result in larger fiber coupling efficiency than would be expected for uniform illumination. Of the light exiting the PCF, 80% was transmitted through the spectrometer input slit; the long-pass filter is the dominant loss. The spectrometer's transmission was found to be 48%, limited by the mirror coatings (aluminum) and the grating efficiency. A mode-locked Ti:Sapphire laser at 900 nm was used to simulate a broadband source at the exit slit; light exiting the slit was coupled into a single mode fiber with 55% efficiency, limited by the spatial mode quality of the beam. The total transmission of the system from the microscope objective lens, through to the spectrally filtered output from the single-mode fiber, was 0.11.

#131463 - $15.00 USD Received 13 Jul 2010; revised 6 Aug 2010; accepted 11 Aug 2010; published 18 Aug 2010

4. Application to quantum dot spectroscopy

The microscope was used to investigate the characteristics of single-photon sources based on optically pumped, self-assembled InAs quantum dots. Principally, this involves optimizing the sample's spectral emission, and measuring $g^{(2)}(\tau)$ to investigate the quantum statistics of emitted photons. A single quantum dot will typically emit more than one spectral component; single-photon emission can be achieved by spectral filtering [5]. To enhance a source's rate and direction of emitted photons, the quantum dot is embedded in a resonant optical microcavity, formed by a pair of distributed Bragg reflectors (DBR) [3,15,16,26]. The microcavity is resonant with one of the dot's spectral components.

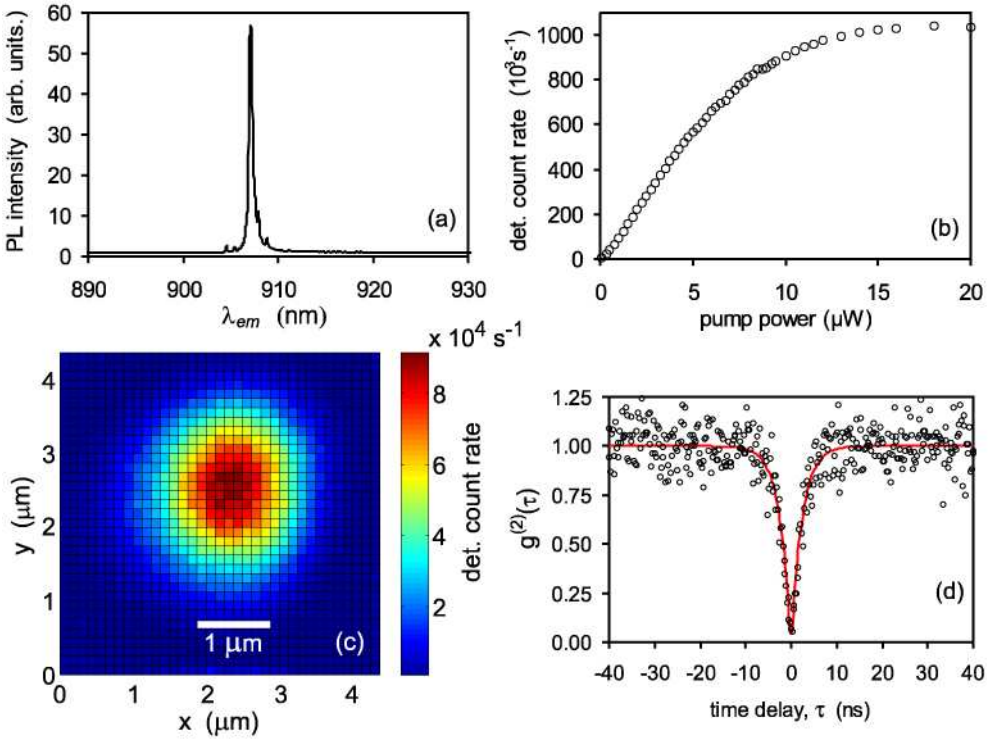

Fig. 3. a) PL emission spectrum of a single quantum dot resonant with 2 μm diameter microcavity. b) Variation in emitted photon flux with pump power; the linear dependence below saturation indicates that the microcavity is resonant with the exciton transition. c) 2D raster scan of emission from a microcavity containing a single dot. d) Correlation histogram, showing $g^{(2)}\left(\tau = 0\right) = 0.05$.

In this work, the cavity was designed to have a resonance at λ_c = 904 nm when etched into a 2 μm diameter pillar [27]; the cavity mirrors are highly reflective over a ~100 nm range around λ_c. 22.5 alternately repeating layers of AlAs (68.2 nm) and GaAs (57.5 nm) were grown on the substrate to form the lower DBR. The λ cavity consists of a layer of low-density QDs sandwiched between two 109.3 nm GaAs layers. A further 12 repeated layers of AlAs and GaAs were grown to form the top DBR. Under high pump power, a pillar microcavity will exhibit a broadband background, filtered by the cavity resonance, the linewidth of which can be used to measure the cavity *Q*. In this work, the pillar microcavity samples had diameter = 2 μm, were pumped by a continuous wave diode laser at λ_p = 802 nm, and showed a cavity *Q* ~1350.

The stochastic nature of the quantum dots' growth process results in a distribution of dot sizes, which results in a spread of λ_{em} over a sample of dots. The sample temperature T_s tunes the emission wavelength of the quantum dot transitions, and also the microcavity resonance

#131463 - $15.00 USD Received 13 Jul 2010; revised 6 Aug 2010; accepted 11 Aug 2010; published 18 Aug 2010

λ_c. As T_s increases both λ_{em} and λ_c redshift, but $d\lambda_{em}/dT_s > d\lambda_c/dT_s$, thus in principal it is possible to achieve $\lambda_{em} = \lambda_c$. The dots' emission is typically quenched when $T_s > 77\,\mathrm{K}$, limiting the practical scope of this technique, although it is noted that single photons from quantum dots have been observed at $T_s > 100\,\mathrm{K}$ [28]. Figure 3a shows the emission spectrum of a single dot resonant with a 2 μm diameter pillar microcavity at $T_s = 10\,\mathrm{K}$, where the emission line intensity was maximized. The emitted photon flux in this feature displays a linear dependence on pump power below saturation (Fig. 3b), showing that this is the dot's exciton transition in resonance with the microcavity [29]. A raster scan image of the photon emission is shown in Fig. 3c, where the FWHM of the detected intensity distribution is 1.65 μm.

To demonstrate the single-photon nature of this source, the exciton transition is selected by the spectrometer (0.11nm bandwidth) and the photons are analyzed by a Hanbury Brown & Twiss (HBT) correlator. Figure 3d presents an example correlation histogram, where $g^{(2)}(\tau = 0) = 0.05$, thus confirming that a single emitter is resonant with the cavity and imaged by the microscope. A simple exponential formula $g^{(2)}(\tau) = 1 - a\exp\left(-|\tau|/t_m\right)$ can describe the data, where t_m is the characteristic decay time and a accounts for the background [30]. Before fitting to the data, this equation for $g^{(2)}(\tau)$ is convolved with a top hat function of width equal to the correlator bin width (223 ps), added to the SPADs' jitter (350 ps per detector, added in quadrature).

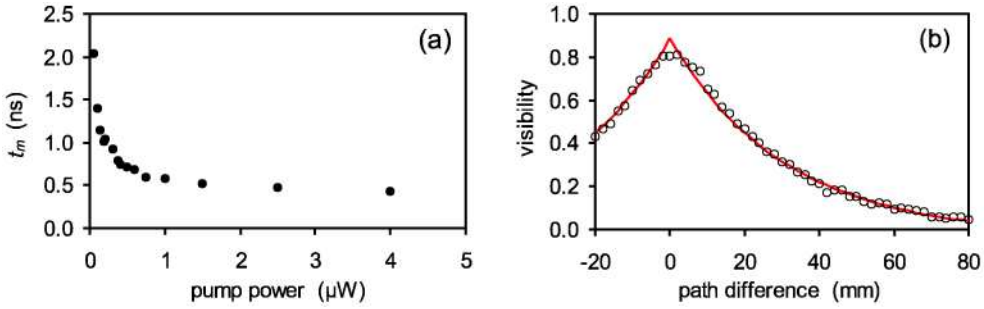

Fig. 4. Characteristic parameters of single photons. a) The decay time t_m, determined by measuring $g^{(2)}(\tau) = 1 - a\exp\left(-|\tau|/t_m\right)$ as a function of pump power. At high pump powers, t_m tends to the spontaneous decay time τ_s = 420 ps. b) Interference fringe visibility as a function of interferometer path difference; the exponential decay yields the coherence length.

A brighter dot was used to illustrate the variation in t_m with pump power, to enable easier data acquisition at low powers. Figure 4a shows that at high pump power, t_m approaches a constant value, the limit being a measure of the dot's spontaneous radiative decay time τ_s = 420 ps. By directing the flux of single photons from this dot to a Michelson interferometer, interference fringes were observed at zero path difference. Fringe visibility was measured for increasing path difference (Fig. 4b), and the exponential decay in visibility is a measure of the photons' coherence length l_c = 30.6 mm, equivalent to a coherence time τ_c = 102 ps. This is some way from the transform limit, where $2\tau_s/\tau_c = 1$ and the photons are completely indistinguishable. Using a tunable laser to near-resonantly excite the quantum dot is expected to get closer to this limit [15,16].

5. Summary

This paper has presented the concept and operation of a fiber-optic confocal microscope that uses the large mode area of an endlessly single mode photonic crystal fiber as the confocal pinhole. The microscope, developed for imaging single emitters in solid-state systems at low temperatures, was designed to maximize detected photon flux while maintaining a working

#131463 - $15.00 USD Received 13 Jul 2010; revised 6 Aug 2010; accepted 11 Aug 2010; published 18 Aug 2010

distance of a few mm. With a magnification of 10, photons are imaged efficiently into the fiber's single mode. When operating at λ ~900 nm, the lateral and axial resolutions were measured to be 1.0 μm and 2.5 μm respectively. The microscope's use was demonstrated by imaging optically pumped single InAs quantum dots in pillar microcavities. Quantum statistics of the PL were investigated by measuring $g^{(2)}(\tau)$, and demonstrated the single-photon nature of the source. The coherence time of the single photons was determined interferometrically.

To tailor the microscope's performance for specific applications, alternative components can be used. Where the polarization of the pump or detected light is critical, then polarization-maintaining large mode area fibers are available and are straightforward to introduce. For applications in the visible wavelength range, high quality objective lenses are readily available and will enable operation free of chromatic aberration.

The endlessly single mode property of our confocal microscope has potential benefits in multiphoton and chromatic microscopy. In two-photon confocal microscopy, the pump and fluorescence light can be confined to a single spatial mode in the same fiber, despite the difference in wavelength. Furthermore, the large mode area of the PCF can alleviate pulse broadening of the pump due to self-phase modulation, thus enabling a single-mode fiber microscope where free space is the more conventional approach. Chromatic confocal microscopy, using a supercontinuum for broadband illumination, could also be fiber-enabled through the use of the endlessly single-mode PCF as the confocal aperture.

Acknowledgements

This work was supported by the UK's National Measurement System Pathfinder Metrology research programme, and by EURAMET project "QuCandela". The research within this EURAMET joint research project leading to these results has received funding from the European Community's Seventh Framework Programme, ERA-NET Plus, under Grant Agreement No. 217257. RH acknowledges support form the UK EPSRC. We thank P. Stavrinou for calculating the DBR microcavity design, R. Murray for stimulating discussions, and G. Lepert for assistance in acquiring data from the semiconductor source.

#131463 - $15.00 USD Received 13 Jul 2010; revised 6 Aug 2010; accepted 11 Aug 2010; published 18 Aug 2010